

## The pion-nucleon sigma term from Lattice QCD

---

**Rajan Gupta,<sup>a,\*</sup> Tanmoy Bhattacharya,<sup>a</sup> Martin Hoferichter,<sup>b</sup> Emanuele Mereghetti,<sup>a</sup>  
Sungwoo Park<sup>a,c</sup> and Boram Yoon<sup>d</sup>**

<sup>a</sup>Los Alamos National Laboratory, Theoretical Division T-2, Los Alamos, NM 87545, USA

<sup>b</sup>Albert Einstein Center for Fundamental Physics, Institute for Theoretical Physics, University of Bern,  
Sidlerstrasse 5, 3012 Bern, Switzerland

<sup>c</sup>Jefferson Lab, 12000 Jefferson Avenue, Newport News, Virginia 23606, USA

<sup>d</sup>Los Alamos National Laboratory, Computer Computational and Statistical Sciences Division, CCS-7, Los  
Alamos, NM 87545, USA

E-mail: [rajan@lanl.gov](mailto:rajan@lanl.gov)

We summarize recent evidence, both from lattice QCD and chiral perturbation theory, that suggests that larger-than-expected excited-state contamination could be the reason for the tension between phenomenological determinations and previous direct lattice-QCD calculations of the pion–nucleon sigma term  $\sigma_{\pi N}$ . In addition, we extend the  $\chi$ PT analysis by calculating the corrections due to including the  $\Delta(1232)$  resonance as an explicit degree of freedom. This correction is found to be small, thereby corroborating the excited-state effects found in the  $\Delta$ -less calculation and the result for  $\sigma_{\pi N}$ .

*The 10th International Workshop on Chiral Dynamics  
15–19 November 2021  
Beijing, China*

---

\*Speaker

## 1. Introduction

In Ref. [1], we proposed a possible resolution to a persistent tension between lattice-QCD and phenomenological determinations of the pion–nucleon  $\sigma$ -term  $\sigma_{\pi N}$ . This quantity describes the coupling of the nucleon to an isosymmetric scalar current comprised of the two lightest quarks and appears prominently in searches for physics beyond the Standard Model whenever scalar currents play a role, e.g., in direct-detection searches for dark matter [2–6], lepton flavor violation in  $\mu \rightarrow e$  conversion in nuclei [7, 8], and electric dipole moments [9–12]. Even though there is no scalar probe in the Standard Model,  $\sigma_{\pi N}$  can still be extracted from data on pion–nucleon ( $\pi N$ ) scattering via the Chang–Dashen low-energy theorem [13, 14]. Such determinations have a long history [15, 16], with all recent determinations converging on a value around 60 MeV, irrespective of whether the  $\pi N$  input is taken from data on pionic atoms [17–23] or low-energy  $\pi N$  cross sections [24]. In contrast, most lattice calculations [25–29] (with the exception of Ref. [30]) prefer a value as low as 40 MeV, producing the tension [31] summarized in Fig. 1 and in the FLAG 2021 report [32]. These lattice calculations can be grouped into those applying the Feynman–Hellmann theorem, in which case the quark-mass derivative of the nucleon mass needs to be controlled very accurately, and via the direct calculation of the three-point function. Reference [1] provided lattice evidence that the mismatch between the direct method and phenomenology can be explained by larger-than-expected multihadron excited-state contamination (ESC). Motivation for such ESC was also presented using chiral perturbation theory ( $\chi$ PT). Here, after a short review of the lattice-immanent arguments given in Sec. 2, we extend the  $\chi$ PT calculation of ESC for the  $\Delta$ -less case presented in Ref. [1] and reviewed in Sec. 3 to include the  $\Delta(1232)$  as an explicit degree of freedom in Sec. 4. The change on including the  $\Delta$  is small and does not change the conclusions, which are summarized in Sec. 5.

## 2. Lattice data

The lattice calculation presented in Ref. [1] constructed Euclidean correlation functions using Wilson-clover fermions on six 2+1+1-flavor ensembles generated using the highly improved staggered quark action [33] by the MILC collaboration [34]. These ensembles include data at  $M_\pi \approx 315, 230, \text{ and } 138 \text{ MeV}$ . To obtain the flavor-diagonal charges  $g_S^q$ , both connected and disconnected diagrams were calculated using the methodology presented in Refs. [35, 36]. Simultaneous fits to the zero momentum nucleon two-point,  $C^{2\text{pt}}$ , and three-point,  $C^{3\text{pt}}$ , functions were made using their spectral decomposition

$$\begin{aligned} C^{2\text{pt}}(\tau; \mathbf{k}) &= \sum_{i=0}^3 |\mathcal{A}_i(\mathbf{k})|^2 e^{-M_i \tau}, \\ C_S^{3\text{pt}}(\tau; t) &= \sum_{i,j=0}^2 \mathcal{A}_i \mathcal{A}_j^* \langle i | \mathcal{S} | j \rangle e^{-M_i t - M_j(\tau-t)}, \end{aligned} \quad (1)$$

keeping four and three states, respectively. Here,  $\tau$  denotes the source–sink separation and  $t$  the time of the operator insertion, while  $\mathcal{A}_i$  are the amplitudes for the creation or annihilation of states by the nucleon interpolating operator.

The important observation was that current lattice data are not precise enough to resolve the excited-state masses  $M_1$  and  $M_2$ . Fits using two strategies,  $\{4, 3^*\}$  (standard fit, wide priors on

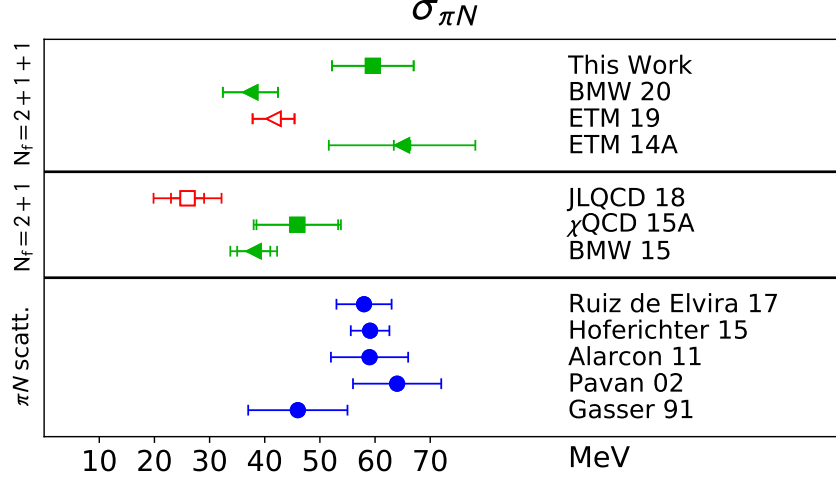


**Figure 1:** Results for  $\sigma_{\pi N} = m_{ud}g_S^{u+d}$  from 2+1- and 2+1+1-flavor lattice calculations. The BMW 20 result from 1+1+1+1-flavor lattices is listed along with 2+1+1-flavor calculations for brevity: the difference is expected to be insignificant. Calculations in the direct approach are indicated by squares and the Feynman–Hellmann method by triangles. The references from which lattice results have been taken are: JLQCD 18 [27],  $\chi$ QCD 15A [26], BMW 15 [25], ETM 14A [30], ETM 19 [28], and BMW 20 [29]. Phenomenological determinations from  $\pi N$  scattering data (blue filled circles) are from Gasser 91 [15], Pavan 02 [16], Alarcon 11 [22], Hoferichter 15 [23], and Ruiz de Elvira 17 [24]. Figure reproduced from Ref. [1].

the  $M_{i>0}$ ) and  $\{4^{N\pi}, 3^*\}$  (excited-state fit, motivated by  $\chi$ PT, with narrow prior for  $M_1$  centered around the noninteracting energy of the almost-degenerate lowest positive-parity multihadron states,  $N(\mathbf{1})\pi(-\mathbf{1})$  or  $N(\mathbf{0})\pi(\mathbf{0})\pi(\mathbf{0})$ ) gave similarly good fits, but vastly different results for  $\sigma_{\pi N}$ . While the standard fit reproduces values around 40 MeV, imposing multihadron ESC as in the  $\{4^{N\pi}, 3^*\}$  fit gave  $\approx 60$  MeV, thus removing the tension with the phenomenological value. The calculation needs validation, e.g., the conclusion is mainly driven by the single physical pion mass ensemble, however, it was supported by an analysis of ESC in  $\chi$ PT, as we will delineate in the following.

### 3. Excited states in chiral perturbation theory

ESC has been studied before using  $\chi$ PT methods [37–39]. Given the subtle chiral expansion of  $\sigma_{\pi N}$ , with chiral loops only suppressed by a single order compared to the tree-level contribution and even subleading loops enhanced due to the presence of the  $\Delta(1232)$  as reflected by large values of the corresponding low-energy constants (LECs)  $c_i$ , we carried out a full next-to-next-to-leading-order (N<sup>2</sup>LO) analysis, including the diagrams shown in Fig. 2. Expressed in terms of ratios of correlation functions  $\mathcal{R}_S(\tau, t)$ , which for  $t, \tau \rightarrow \infty$  yield  $\sigma_{\pi N}$ , we find

$$\begin{aligned} \mathcal{R}^{(1)}(\tau, t) = & \frac{3g_A^2 M_\pi^2}{8F_\pi^2 L^3} \sum_{\mathbf{k}} \frac{\mathbf{k}^2}{E_\pi^4} \left[ 1 - e^{-E_{N\pi}t} - e^{-E_{N\pi}t_B} + \frac{1}{2}e^{-E_{N\pi}\tau} + \frac{1}{4}e^{-2E_\pi t} + \frac{1}{4}e^{-2E_\pi t_B} \right] \\ & - \frac{3M_\pi^2}{32F_\pi^2 L^3} \frac{1}{\sum_{\mathbf{k}} \frac{1}{E_\pi^2}} \left( e^{-2E_\pi t} + e^{-2E_\pi t_B} \right), \end{aligned}$$

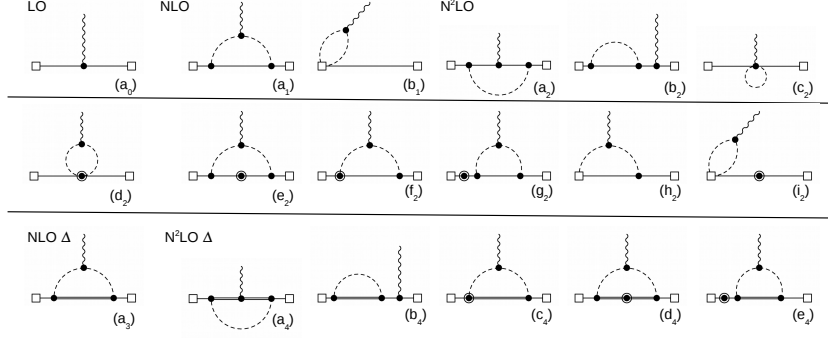


**Figure 2:** Corrections to the scalar charge in  $\chi$ PT. Empty and full squares denote, respectively, insertions of the LO and NLO expansion of the source fields  $\mathcal{N}$  and  $\tilde{\mathcal{N}}$ . Plain, dashed, and wavy lines denote, nucleons, pions, and an insertion of the scalar source. Dots and circled dots denote LO and NLO vertices in the chiral Lagrangian. Diagrams  $(h_2)$  and  $(i_2)$  are representative of  $\text{N}^2\text{LO}$  corrections arising from the chiral expansion of  $\mathcal{N}$ , which only produces negligible  $\text{N}^2\text{LO}$  recoil corrections. The diagrams in the last row show the corrections induced by the  $\Delta$  baryon, at NLO (diagram  $(a_3)$ ) and  $\text{N}^2\text{LO}$  (diagrams  $(a_4)$  to  $(e_4)$ ).

$$\begin{aligned} \mathcal{R}_{c_i}^{(2)}(\tau, t) = & -\frac{3M_\pi^2}{4F_\pi^2} \frac{1}{L^3} \sum_{\mathbf{k}} \frac{1}{E_\pi^3} \left( (c_2 + 2c_3) E_\pi^2 + (2c_1 - c_3) M_\pi^2 \right) \left[ 1 - \frac{1}{2} e^{-2E_\pi t} - \frac{1}{2} e^{-2E_\pi t_B} \right] \\ & + \frac{3M_\pi^2}{F_\pi^2} \frac{1}{L^3} \sum_{\mathbf{k}} \frac{1}{E_\pi} c_1, \end{aligned} \quad (2)$$

for the next-to-leading-order (NLO) result  $\mathcal{R}^{(1)}$  and the by far most sizable  $\text{N}^2\text{LO}$  correction  $\mathcal{R}_{c_i}^{(2)}$  involving the LECs  $c_i$ . The notation for the energies that appear in the sum over discrete momenta  $\mathbf{k} = 2\pi\mathbf{n}/L$  is  $E_\pi = \sqrt{\mathbf{k}^2 + M_\pi^2}$ ,  $\tilde{E}_N = \sqrt{M_N^2 + \mathbf{k}^2} - M_N$ ,  $E_{N\pi} = E_\pi + \tilde{E}_N$ ,  $M_N$  and  $M_\pi$  are the full nucleon and pion mass at the corresponding quark mass in the lattice simulation, and the time difference  $\tau - t$  is denoted by  $t_B$ . Note that  $E_{N\pi}$  subsumes some of the  $\text{N}^2\text{LO}$  recoil corrections. For the remaining contributions as well as finite-volume corrections, evaluated as the difference of the ground-state contribution in Eq. (2) to the continuum result [40], we refer to Ref. [1].

Using the values for the  $c_i$  from Refs. [41, 42], we find that both contributions in Eq. (2) produce large, negative corrections, that make  $\sigma_{\pi N}$  too small if these ESC are not taken into account. Depending on the details of the lattice ensemble in question, we find that NLO and  $\text{N}^2\text{LO}$  contributions can each generate up to  $-10$  MeV at  $t = \tau/2 \sim (0.5-0.7)$  fm. The combined effect is to reduce the  $\approx 60$  MeV value on the physical mass ensemble to  $\approx 40$  MeV. Previous calculations using the direct method did not include these multihadron states in their analysis [32], thus creating the tension between direct lattice calculations of  $\sigma_{\pi N}$  and phenomenology. A similar argument about the relevance of these multihadron ESC also applies to the Feynman–Hellmann method. A standard worry, however, in such  $\chi$ PT analyses is that the results need to be applied at scales at which the convergence of the heavy-baryon expansion is not guaranteed. Here we extend the analysis by considering the effect of including the  $\Delta(1232)$  as an explicit degree of freedom to gauge the stability of the chiral expansion. These new results are presented in the next section.

#### 4. Including the $\Delta(1232)$ resonance as explicit degree of freedom

The first contribution from the  $\Delta(1232)$  arises at NLO and is shown in diagram ( $a_3$ ) in Fig. 2. We find

$$\begin{aligned} \mathcal{R}_\Delta^{(1)}(\tau, t) = & \frac{h_A^2 M_\pi^2}{6F_\pi^2} \left(1 - \frac{\epsilon}{3}\right) \frac{1}{L^3} \sum_{\mathbf{k}} \frac{\mathbf{k}^2}{E_\pi^3 (E_\pi + \Delta)^2} \left\{ 2(2E_\pi + \Delta) - (3E_\pi + \Delta) \left( e^{-2E_\pi t} + e^{-2E_\pi t_B} \right) \right. \\ & \left. + 2E_\pi e^{-(E_\pi + \Delta)(t + t_B)} + 4E_\pi^2 \left( e^{-E_\pi t} \frac{e^{-E_\pi t} - e^{-\Delta t}}{E_\pi - \Delta} + e^{-E_\pi t_B} \frac{e^{-E_\pi t_B} - e^{-\Delta t_B}}{E_\pi - \Delta} \right) \right\}, \end{aligned} \quad (3)$$

written in a form that makes the cancellation of the singularities at  $E_\pi = \Delta = M_\Delta - M_N$  apparent. At NLO, the  $\Delta$ -nucleon mass splitting in Eq. (3) should be interpreted strictly in the chiral limit,  $\Delta = \Delta^{(0)} = M_\Delta^{(0)} - M_N^{(0)}$ . Here  $\epsilon = (4 - d)/2$  is the regulator in dimensional regularization, as needed to reproduce the continuum result from Eq. (3), and  $h_A$  denotes the  $\pi N \Delta$  coupling in the conventions of Ref. [43]. The finite-volume corrections can again be obtained by comparing the ground-state contribution to the continuum, i.e., momentum sums versus integrals, leading to

$$\Delta_L^{(1), \Delta} \sigma_{\pi N} = \frac{h_A^2 M_\pi^2}{6\pi^2 F_\pi^2} \sum_{\mathbf{n} \neq 0} \int_0^\infty d\lambda \left[ 3K_0(L\sqrt{\beta}|\mathbf{n}|) - \sqrt{\beta}L|\mathbf{n}|K_1(L\sqrt{\beta}|\mathbf{n}|) \right], \quad (4)$$

with  $\beta = \lambda^2 + 2\lambda\Delta + M_\pi^2$  and Bessel functions  $K_0, K_1$ .

N<sup>2</sup>LO corrections arise from recoil corrections to the  $\Delta$  propagator and to the  $\Delta$ -nucleon vertices, as well as from the LEC  $c_1^\Delta$ . The latter contributes in two ways, by mediating the coupling of the scalar charge to the  $\Delta$  baryon and by providing a quark-mass dependent correction to the  $\Delta$  mass. Diagrams ( $d_4$ ) and ( $e_4$ ) can be absorbed by shifting

$$\begin{aligned} \Delta \rightarrow \tilde{E}_\Delta & \equiv \sqrt{\left( M_N^{(0)} + \Delta^{(0)} - 4M_\pi^2 c_1^\Delta \right)^2 + \mathbf{k}^2} - \left( M_N^{(0)} - 4M_\pi^2 c_1 \right) \\ & = \Delta^{(0)} - 4M_\pi^2 (c_1^\Delta - c_1) + \frac{\mathbf{k}^2}{2M_N^{(0)}} + \mathcal{O}(M_N^{-2}), \end{aligned} \quad (5)$$

in the NLO contribution (3).  $c_1$  and  $c_1^\Delta$  quantify pure explicit-symmetry-breaking terms, in such a way that the nucleon and  $\Delta$  becoming degenerate in the large- $N_c$  limit strongly suggesting  $c_1 = c_1^\Delta$  up to  $1/N_c$  corrections [43]. Effectively, we capture these corrections by using the physical values of the nucleon and  $\Delta$  masses in  $\tilde{E}_\Delta$  and in Eq. (3).

The remaining N<sup>2</sup>LO corrections are given by diagrams ( $a_4$ ), ( $b_4$ ), and ( $c_4$ ) and by analogous corrections to the two-point function, which yield

$$\begin{aligned} \mathcal{R}_\Delta^{(2)}(\tau, t) = & \frac{2h_A^2 M_\pi^2}{3F_\pi^2} \left(1 - \frac{\epsilon}{3}\right) \left( \frac{1}{M_N} - 4(c_1^\Delta - c_1) \right) \\ & \times \frac{1}{L^3} \sum_{\mathbf{k}} \frac{\mathbf{k}^2}{E_\pi (E_\pi + \Delta)^2} \left[ 1 - e^{-(E_\pi + \Delta)t} - e^{-(E_\pi + \Delta)t_B} + e^{-(E_\pi + \Delta)(t + t_B)} \right] \\ & + \frac{2h_A^2 M_\pi^2}{3F_\pi^2 M_N} \left(1 - \frac{\epsilon}{3}\right) \frac{1}{L^3} \sum_{\mathbf{k}} \frac{1}{E_\pi} \left[ 1 - \frac{1}{2} e^{-2E_\pi t} - \frac{1}{2} e^{-2E_\pi t_B} \right]. \end{aligned} \quad (6)$$

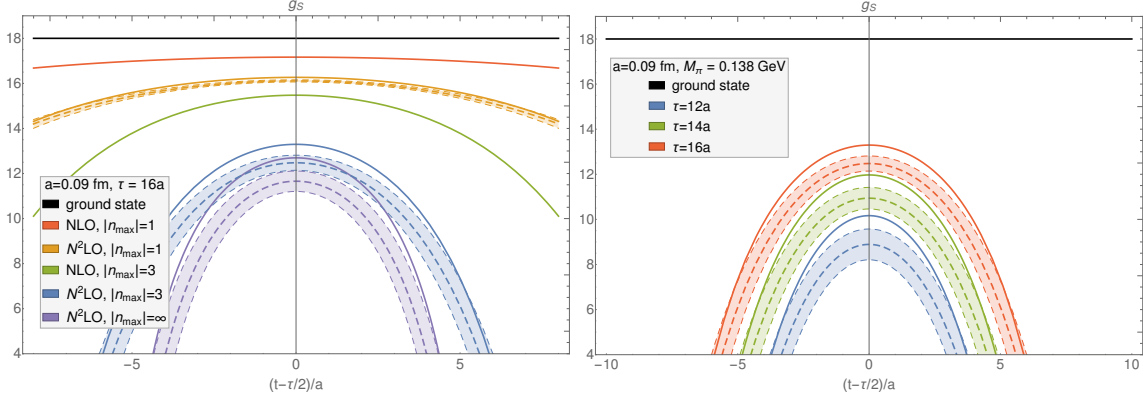


**Figure 3:** (Left) ESC from different truncations to the isoscalar scalar charge  $g_S$  in  $\chi$ PT. (Right) Estimates for  $R_S(\tau, t)$  from the N<sup>2</sup>LO analysis for the a09m130 ensemble. In both cases, the dashed bands indicate the outcome of the full N<sup>2</sup>LO analysis including the  $\Delta(1232)$ , in comparison to the  $\Delta$ -less results using solid lines. The figure generalizes Fig. 6 in Ref. [1].

To obtain these expressions, we have chosen a renormalization scheme that reproduces the continuum results from Ref. [44], ensuring consistency with the LECs from Ref. [43]. The last line of Eq. (6) leads to a shift in the couplings  $c_2 + 2c_3$  in Eq. (2) by  $\Delta(c_2 + 2c_3) = -8h_A^2/(9M_N)$ . The first line contains a recoil correction and a correction proportional to  $c_1^\Delta - c_1$ . As discussed above, the latter is expected to vanish in the large- $N_c$  limit.

Equation (3) is evaluated numerically with the resummed shift (5) and the physical value of the  $\Delta$ -nucleon mass splitting. Further, we vary  $c_1 - c_1^\Delta$  between  $\pm|c_1|/N_c$  as an estimate of the corresponding uncertainty, leading to the bands in Fig. 3 for the full N<sup>2</sup>LO analysis including the  $\Delta(1232)$  baryon. For comparison, the results from the  $\Delta$ -less calculation are shown by solid lines, both for different truncations in the chiral order and sum over momenta  $\mathbf{k}$  (left) and source-sink separations (right). In particular, the figure illustrates that the corrections beyond the N<sup>2</sup>LO  $\Delta$ -less results are small, much smaller than the shift between NLO and N<sup>2</sup>LO results. These findings indicate that the chiral expansion is reasonably stable, with the main effects indeed captured by the leading-loop contributions and the  $\Delta$ -enhanced corrections from the  $c_i$  that were already included in Ref. [1].

## 5. Conclusions

We have summarized the main arguments from Ref. [1] that provide a resolution of the tension between phenomenological determinations of  $\sigma_{\pi N}$  and direct lattice calculations. We demonstrated the impact of ESC in both the lattice calculation and in  $\chi$ PT up to N<sup>2</sup>LO. Here we have extended the  $\chi$ PT calculation to include the  $\Delta(1232)$  resonance as an explicit degree of freedom to assess the stability of the chiral expansion, and find that for  $\sigma_{\pi N}$  the impact is remarkably small, thereby corroborating the conclusions from the  $\Delta$ -less heavy-baryon analysis presented in Ref. [1].

## Acknowledgments

M.H. acknowledges financial support by the Swiss National Science Foundation (Project No. PCEFP2\_181117). T.B. and R.G. were partly supported by the DOE HEP under Award No. DE-AC52-06NA25396. T.B., R.G., E.M., S.P., and B.Y. were partly supported by the LANL LDRD program.

## References

- [1] R. Gupta, S. Park, M. Hoferichter, E. Mereghetti, B. Yoon and T. Bhattacharya, *Pion–Nucleon Sigma Term from Lattice QCD*, *Phys. Rev. Lett.* **127** (2021) 242002 [2105.12095].
- [2] A. Bottino, F. Donato, N. Fornengo and S. Scopel, *Implications for relic neutralinos of the theoretical uncertainties in the neutralino nucleon cross-section*, *Astropart. Phys.* **13** (2000) 215 [hep-ph/9909228].
- [3] A. Bottino, F. Donato, N. Fornengo and S. Scopel, *Size of the neutralino nucleon cross-section in the light of a new determination of the pion nucleon sigma term*, *Astropart. Phys.* **18** (2002) 205 [hep-ph/0111229].
- [4] J.R. Ellis, K.A. Olive and C. Savage, *Hadronic Uncertainties in the Elastic Scattering of Supersymmetric Dark Matter*, *Phys. Rev. D* **77** (2008) 065026 [0801.3656].
- [5] A. Crivellin, M. Hoferichter and M. Procura, *Accurate evaluation of hadronic uncertainties in spin-independent WIMP-nucleon scattering: Disentangling two- and three-flavor effects*, *Phys. Rev. D* **89** (2014) 054021 [1312.4951].
- [6] M. Hoferichter, P. Klos, J. Menéndez and A. Schwenk, *Improved limits for Higgs-portal dark matter from LHC searches*, *Phys. Rev. Lett.* **119** (2017) 181803 [1708.02245].
- [7] V. Cirigliano, R. Kitano, Y. Okada and P. Tuzon, *On the model discriminating power of  $\mu \rightarrow e$  conversion in nuclei*, *Phys. Rev. D* **80** (2009) 013002 [0904.0957].
- [8] A. Crivellin, M. Hoferichter and M. Procura, *Improved predictions for  $\mu \rightarrow e$  conversion in nuclei and Higgs-induced lepton flavor violation*, *Phys. Rev. D* **89** (2014) 093024 [1404.7134].
- [9] J. Engel, M.J. Ramsey-Musolf and U. van Kolck, *Electric Dipole Moments of Nucleons, Nuclei, and Atoms: The Standard Model and Beyond*, *Prog. Part. Nucl. Phys.* **71** (2013) 21 [1303.2371].
- [10] J. de Vries and U.-G. Meißner, *Violations of discrete space–time symmetries in chiral effective field theory*, *Int. J. Mod. Phys. E* **25** (2016) 1641008 [1509.07331].
- [11] J. de Vries, E. Mereghetti, C.-Y. Seng and A. Walker-Loud, *Lattice QCD spectroscopy for hadronic CP violation*, *Phys. Lett. B* **766** (2017) 254 [1612.01567].

- [12] N. Yamanaka, B.K. Sahoo, N. Yoshinaga, T. Sato, K. Asahi and B.P. Das, *Probing exotic phenomena at the interface of nuclear and particle physics with the electric dipole moments of diamagnetic atoms: A unique window to hadronic and semi-leptonic CP violation*, *Eur. Phys. J. A* **53** (2017) 54 [1703.01570].
- [13] T.P. Cheng and R.F. Dashen, *Is  $SU(2) \times SU(2)$  a better symmetry than  $SU(3)$ ?*, *Phys. Rev. Lett.* **26** (1971) 594.
- [14] L.S. Brown, W.J. Pardee and R.D. Peccei, *Adler-Weisberger theorem reexamined*, *Phys. Rev. D* **4** (1971) 2801.
- [15] J. Gasser, H. Leutwyler and M.E. Sainio, *Sigma term update*, *Phys. Lett. B* **253** (1991) 252.
- [16] M.M. Pavan, I.I. Strakovsky, R.L. Workman and R.A. Arndt, *The Pion nucleon  $\Sigma$  term is definitely large: Results from a G.W.U. analysis of  $\pi N$  scattering data*, *PiN Newslett.* **16** (2002) 110 [hep-ph/0111066].
- [17] T. Strauch, F.D. Amaro, D.F. Anagnostopoulos, P. Bühler, D.S. Covita, H. Gorke et al., *Pionic deuterium*, *Eur. Phys. J. A* **47** (2011) 88 [1011.2415].
- [18] M. Hennebach, D.F. Anagnostopoulos, A. Dax, H. Fuhrmann, D. Gotta, A. Gruber et al., *Hadronic shift in pionic hydrogen*, *Eur. Phys. J. A* **50** (2014) 190 [1406.6525].
- [19] A. Hirtl, D.F. Anagnostopoulos, D.S. Covita, H. Fuhrmann, H. Gorke, D. Gotta et al., *Redetermination of the strong-interaction width in pionic hydrogen*, *Eur. Phys. J. A* **57** (2021) 70.
- [20] V. Baru, C. Hanhart, M. Hoferichter, B. Kubis, A. Nogga and D.R. Phillips, *Precision calculation of the  $\pi^-$  deuteron scattering length and its impact on threshold  $\pi N$  scattering*, *Phys. Lett. B* **694** (2011) 473 [1003.4444].
- [21] V. Baru, C. Hanhart, M. Hoferichter, B. Kubis, A. Nogga and D.R. Phillips, *Precision calculation of threshold  $\pi^- d$  scattering,  $\pi N$  scattering lengths, and the GMO sum rule*, *Nucl. Phys. A* **872** (2011) 69 [1107.5509].
- [22] J.M. Alarcón, J. Martin Camalich and J.A. Oller, *The chiral representation of the  $\pi N$  scattering amplitude and the pion-nucleon sigma term*, *Phys. Rev. D* **85** (2012) 051503(R) [1110.3797].
- [23] M. Hoferichter, J. Ruiz de Elvira, B. Kubis and U.-G. Meißner, *High-Precision Determination of the Pion–Nucleon  $\sigma$  Term from Roy–Steiner Equations*, *Phys. Rev. Lett.* **115** (2015) 092301 [1506.04142].
- [24] J. Ruiz de Elvira, M. Hoferichter, B. Kubis and U.-G. Meißner, *Extracting the  $\sigma$ -term from low-energy pion–nucleon scattering*, *J. Phys. G* **45** (2018) 024001 [1706.01465].
- [25] BUDAPEST-MARSEILLE-WUPPERTAL COLLABORATION collaboration, *Lattice computation of the nucleon scalar quark contents at the physical point*, *Phys. Rev. Lett.* **116** (2016) 172001 [1510.08013].



- [26]  $\chi$ QCD collaboration,  $\pi N$  and strangeness sigma terms at the physical point with chiral fermions, *Phys. Rev. D* **94** (2016) 054503 [[1511.09089](#)].
- [27] JLQCD collaboration, Nucleon charges with dynamical overlap fermions, *Phys. Rev. D* **98** (2018) 054516 [[1805.10507](#)].
- [28] ETM collaboration, Nucleon axial, tensor, and scalar charges and  $\sigma$ -terms in lattice QCD, *Phys. Rev. D* **102** (2020) 054517 [[1909.00485](#)].
- [29] BMWc collaboration, *Ab-initio calculation of the proton and the neutron's scalar couplings for new physics searches*, [2007.03319](#).
- [30] C. Alexandrou, V. Drach, K. Jansen, C. Kallidonis and G. Koutsou, Baryon spectrum with  $N_f = 2 + 1 + 1$  twisted mass fermions, *Phys. Rev. D* **90** (2014) 074501 [[1406.4310](#)].
- [31] M. Hoferichter, J. Ruiz de Elvira, B. Kubis and U.-G. Meißner, Remarks on the pion–nucleon  $\sigma$ -term, *Phys. Lett. B* **760** (2016) 74 [[1602.07688](#)].
- [32] Y. Aoki et al., *FLAG Review 2021*, [2111.09849](#).
- [33] HPQCD, UKQCD collaboration, Highly improved staggered quarks on the lattice, with applications to charm physics, *Phys. Rev. D* **75** (2007) 054502 [[hep-lat/0610092](#)].
- [34] MILC collaboration, Lattice QCD ensembles with four flavors of highly improved staggered quarks, *Phys. Rev. D* **87** (2013) 054505 [[1212.4768](#)].
- [35] PNDME collaboration, Iso-vector and Iso-scalar Tensor Charges of the Nucleon from Lattice QCD, *Phys. Rev. D* **92** (2015) 094511 [[1506.06411](#)].
- [36] R. Gupta, Y.-C. Jang, B. Yoon, H.-W. Lin, V. Cirigliano and T. Bhattacharya, Isovector Charges of the Nucleon from 2+1+1-flavor Lattice QCD, *Phys. Rev. D* **98** (2018) 034503 [[1806.09006](#)].
- [37] O. Bär, Nucleon-pion-state contribution to nucleon two-point correlation functions, *Phys. Rev. D* **92** (2015) 074504 [[1503.03649](#)].
- [38] B.C. Tiburzi, Chiral Corrections to Nucleon Two- and Three-Point Correlation Functions, *Phys. Rev. D* **91** (2015) 094510 [[1503.06329](#)].
- [39] O. Bär, Nucleon-pion-state contribution in lattice calculations of the nucleon charges  $g_A$ ,  $g_T$  and  $g_S$ , *Phys. Rev. D* **94** (2016) 054505 [[1606.09385](#)].
- [40] S.R. Beane, Nucleon masses and magnetic moments in a finite volume, *Phys. Rev. D* **70** (2004) 034507 [[hep-lat/0403015](#)].
- [41] M. Hoferichter, J. Ruiz de Elvira, B. Kubis and U.-G. Meißner, Matching pion–nucleon Roy–Steiner equations to chiral perturbation theory, *Phys. Rev. Lett.* **115** (2015) 192301 [[1507.07552](#)].

- [42] M. Hoferichter, J. Ruiz de Elvira, B. Kubis and U.-G. Meißner, *Roy–Steiner-equation analysis of pion–nucleon scattering*, *Phys. Rept.* **625** (2016) 1 [[1510.06039](#)].
- [43] D. Siemens et al., *Reconciling threshold and subthreshold expansions for pion–nucleon scattering*, *Phys. Lett. B* **770** (2017) 27 [[1610.08978](#)].
- [44] D. Siemens, *Elastic pion–nucleon scattering in chiral perturbation theory: Explicit  $\Delta(1232)$  degrees of freedom*, [2001.03906](#).